Supplementary material for

Polysulfone–Chitosan Hybrids *via* Imine Chemistry: A Versatile Strategy for Functional Bioactive Materials

Oana Dumbrava*, Daniela Ailincai, Alexandru Anisiei, Irina Rosca, Daniela Rusu, Andrei Dascalu, Iuliana Stoica, Anca Filimon, Luminita Marin*

"Petru Poni" Institute of Macromolecular Chemistry, Iasi, Romania

*dumbrava.oana@icmpp.ro, *lmarin@icmpp.ro

Table of content

Table S3. Roughness average (R.a.) values in nm of the investigated samples, measured on surfaces of 5 × 5 μm^2 and 10 x 10 μm^2

Table S4. Surface free energy values (γ_{sv}) and disperse and polar components (γ_{sv}^{d}, γ_{sv}^{p}) for the investigated coatings in mJ/m^2

Table S5. Surface parameters of the investigated materials based on the sorption/desorption isotherms: sorption capacity (% d.b.), average pore size, specific surface area (m^2/g) and the amount of water retained in the monolayer (g/g).

1.1 Determination of chitosan's molecular weight by viscometry

A series of solutions with different concentrations (0.02, 0.04, 0.06, and 0.08 g/dL) were prepared using a 0.2M sodium acetate and 2% acetic acid mixture. The flow time of each solution (t_i), as well as the solvent alone (t_0), was measured using an Ubbelohde viscometer. Relative viscosity (η_{rel}), specific viscosity (η_{sp}) and reduced viscosity (η_{red}) were then determined, and the reduced viscosity was plotted as a function of concentration (c).

$$\eta_{rel} = \frac{t_i}{t_0}$$

$$\eta_{sp} = \eta_{rel} - 1$$

$$\eta_{red} = \frac{\eta_{sp}}{c}$$

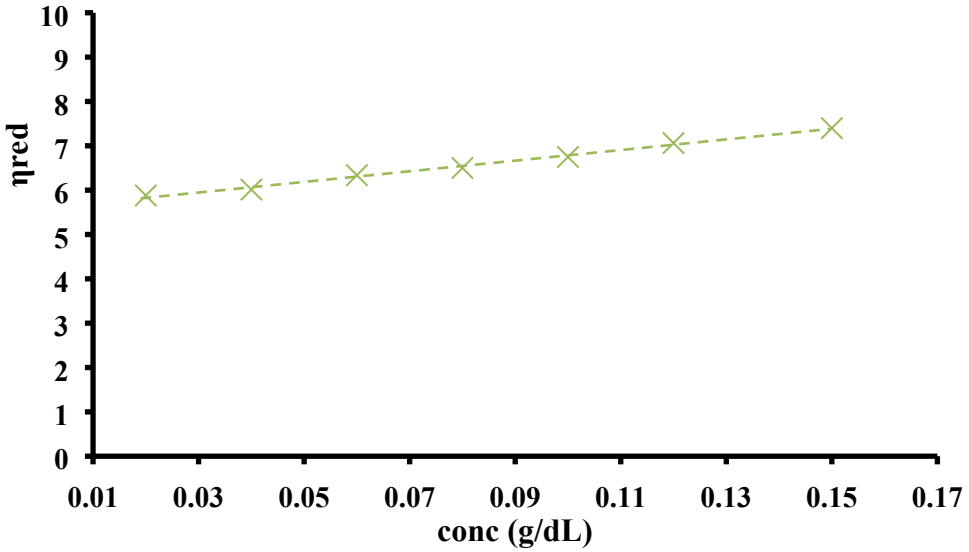

Fig. S1. Determination of molecular weight of chitosan by viscosimetry

The Mark-Houwink equation ($\eta_{in} = k * M_v^a$, where k and a are constants) was applied in order to correlate the reduced viscosity at zero concentration with the molecular weight of chitosan. At 25 °C, for the used dilution system and for a DD of 85±3%, k constant was equal to $74 \cdot 10^{-5}$ and a to 0.76.

1.2 Determination of chitosan's degree of acetylation by ^{1}H-NMR

The degree of acetylation (DA) of chitosan used in this study was calculated by registering its ^{1}H-NMR spectrum in deuterium oxide solution (acidified with 5 µL HCl). The following equation was applied:

$$DA(\%) = \frac{\frac{1}{3} \cdot I_{CH3}}{\frac{1}{6} \cdot I_{(H2-H6)}}$$

where I_{CH3} is the integral value corresponding to the peak located at 1.98 ppm and I_{H2-H6} is the integral value of the signals located between 3.83 and 3.1 ppm.

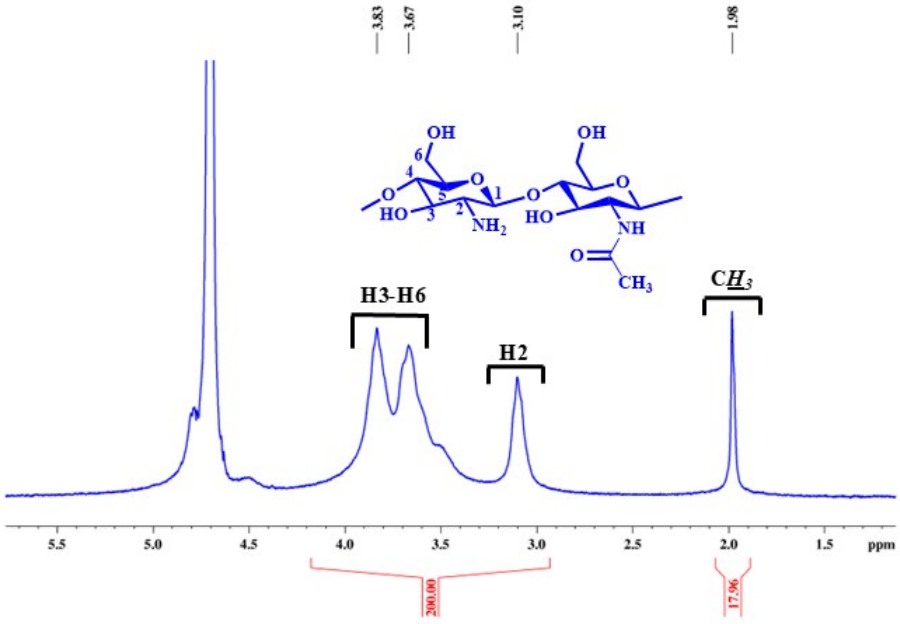

Fig. S2. ^{1}H-NMR spectrum of chitosan recorded in D_2O+HCl

Confirmation of the chemical modification of polysulfone

The successful functionalization of polysulfone with chloromethyl and aldehyde groups, respectively, was confirmed by ^{1}H-NMR and IR spectroscopy. Chloromethylation of PSF took place mainly at the *ortho* position of the B ring of PSF and the two protons of this functional group are observed in the ^{1}H-NMR spectrum as a signal at 4.54 ppm (Figure 2). Moreover, the signals characteristic to the protons from the substituted ring B appear in the ^{1}H-NMR spectra as three peaks, at 7.37, 7.18-7.16 and 6.85-6.83 ppm, while the signals assigned to the protons from the unsubstituted A ring appear as two doublets, at 7.24 and 6.95-6.94 ppm. The protons in the diarylsulfone unit lead to the appearance in ^{1}H-NMR spectrum of two sets of multiplets at 7.88–7.85 and 7.04–7.00 ppm, respectively, while the ones from the isopropyl group lead to the presence of a sharp singlet at 1.71 ppm. The degree of substitution (DS) of CMPSF, calculated from ^{1}H-NMR by applying equation (S1), was found to be 0.9 chloromethyl groups per monomeric unit. The full assignment of the peaks from the ^{1}H NMR spectrum is given in the synthesis part and is in agreement with previously reported data [1].

$$DS = \frac{I_{CH2Cl}}{I_{3C,3D}} \cdot 2 \qquad \text{(S1)}$$

where I_{CH2Cl} is the integral value corresponding to the (–CH_2Cl) peak at 4.54 ppm and $I_{3C,\,3D}$ is the integral value of the multiplet at 7.88–7.85, corresponding to the 4 protons from the C and D aromatic rings, adjacent to the sulfone group.

Chloromethylated polysulfone was further used as a precursor in the Williamson etherification. In the ^{1}H-NMR spectrum of FPSF the peaks for newly introduced benzaldehyde group appear at 9.82-9.81 (-C*H*O), 7.72-7.67 (H-3E) and 6.851-6.80 (H-2E) ppm. Moreover, as a result of the substitution of the CI atom with the p-hydroxy benzaldehyde residue, the signal corresponding to the two protons in the methylene bridge appears in the ^{1}H-RMN spectrum of the formylated polysulfone at 5.06-5.04 ppm because the oxygen atom in the vicinity of the two protons is more electronegative than chlorine, depleting the C-H bonds in electrons and thus unshielding the respective protons. Because of this, the protons in CH_2O resonate at a higher frequency, corresponding to a lower chemical shift of 5.06-5.04 ppm. Also, the absence of the signal at 4.54 ppm in the formylated polysulfone spectrum highlights the total conversion of the

chloromethylated polysulfone into the formylated polysulfone, through the Williamson etherification reaction. The degree of substitution was calculated from ^{1}H-NMR using equation (S2) and was found to be 0.9 benzaldehyde groups per monomeric units, the same as the DS of CMPSF:

$$DS = \frac{I_{CH2-O-}}{I_{CHO}} \cdot 2 \qquad \text{(S2)}$$

where $I_{\underline{CH2}\text{-O-}}$ is the integral value for the two protons of the etheric bridge (5.06-5.04 ppm) and $I_{C\underline{H}O}$ is the integral value for the proton of the aldehyde group (9.82-9.81 ppm).

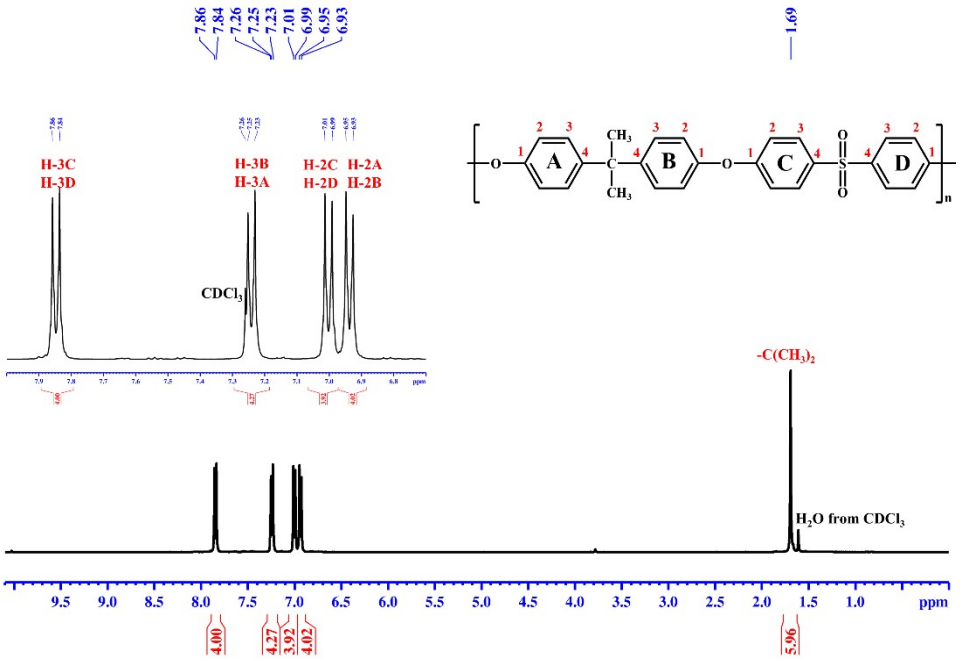

a)

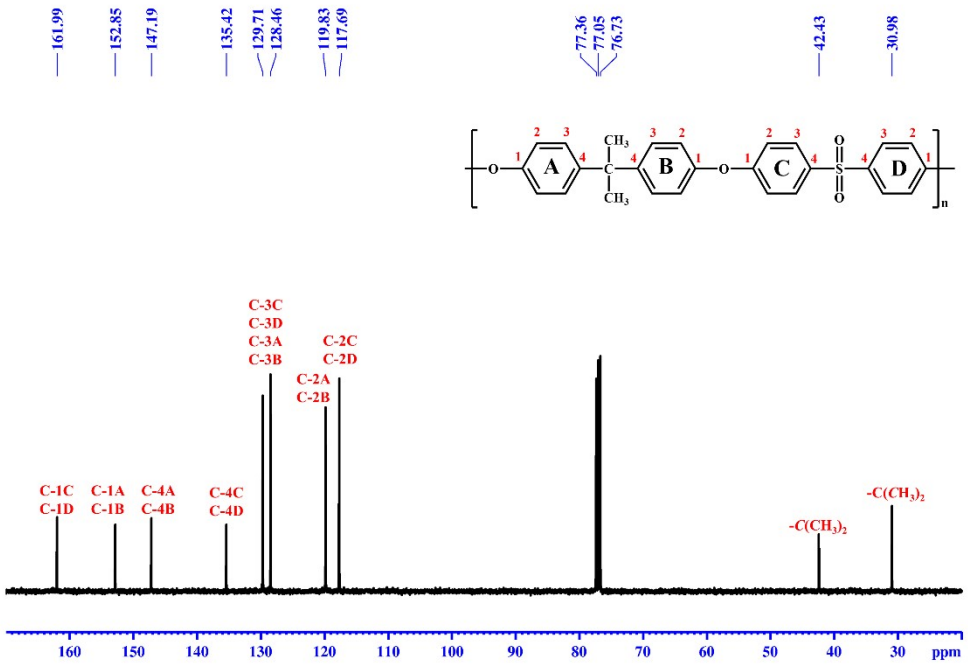
161.99
152.85
147.19
135.42
129.71
128.46
119.83
117.69
77.36
77.05
76.73
42.43
30.98
A
B
C
D
C-3C
C-3D
C-3A
C-3B
C-2C
C-2D
C-2A
C-2B
C-1C
C-1D
C-1A
C-1B
C-4A
C-4B
C-4C
C-4D
-C(CH3)2
-C(CH3)2
160
150
140
130
120
110
100
90
80
70
60
50
40
30
ppm

b)

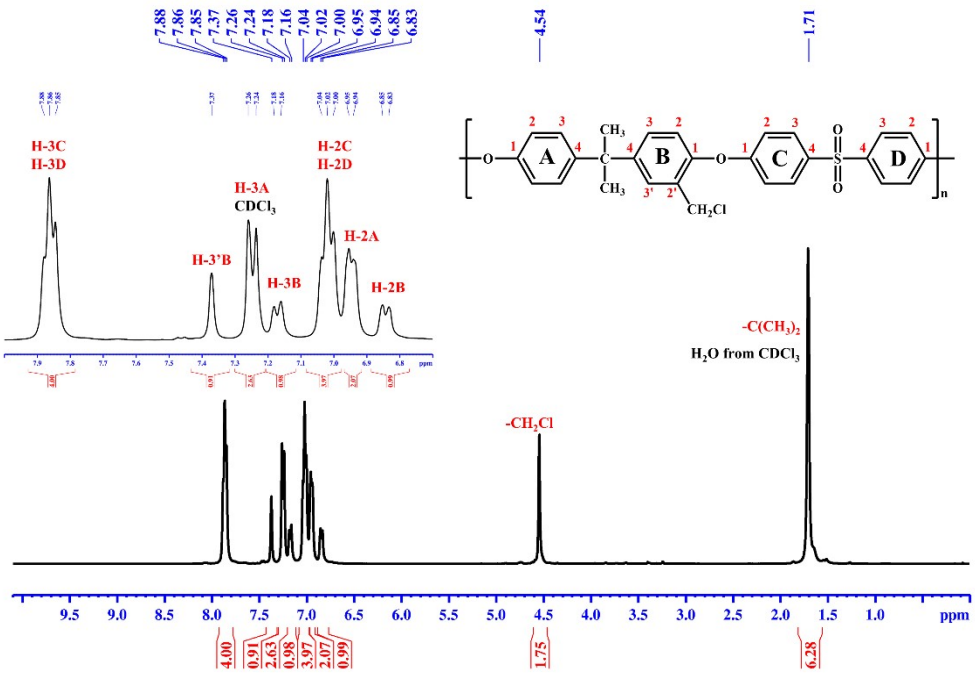
7.88
7.86
7.85
7.37
7.26
7.24
7.18
7.16
7.04
7.02
7.00
6.95
6.94
6.85
6.83
4.54
1.71
A
B
C
D
CH2Cl
H-3C
H-3D
H-3A
CDCl3
H-3'B
H-3B
H-2C
H-2D
H-2A
H-2B
-C(CH3)2
H2O from CDCl3
-CH2Cl
9.5
9.0
8.5
8.0
7.5
7.0
6.5
6.0
5.5
5.0
4.5
4.0
3.5
3.0
2.5
2.0
1.5
1.0
ppm
4.00
0.91
2.63
0.98
3.97
2.07
0.99
1.75
6.28

c)

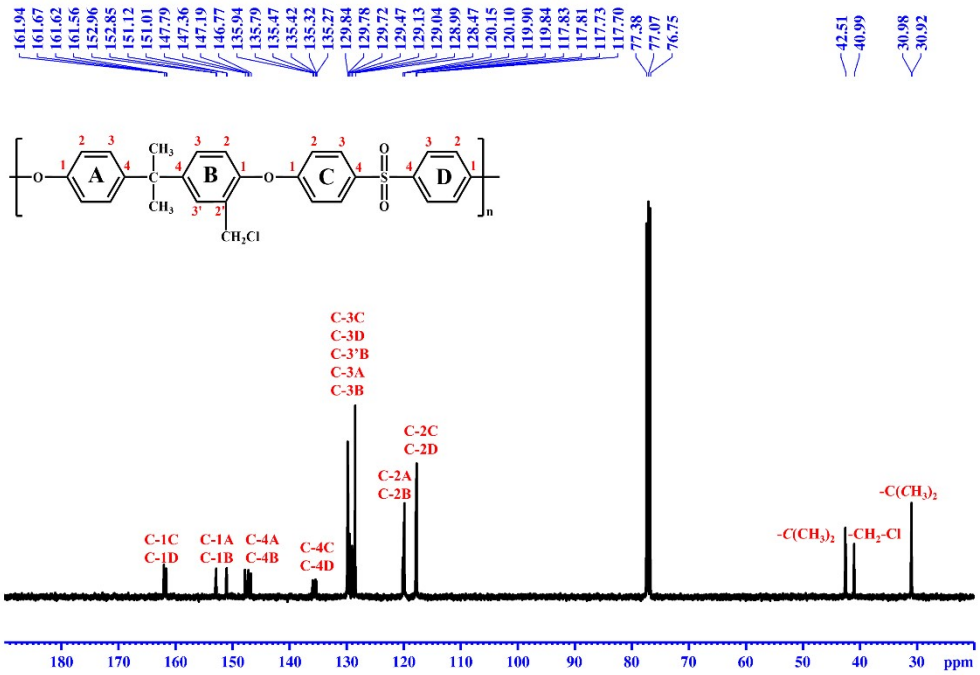
161.94
161.67
161.62
161.56
152.96
152.85
151.12
151.01
147.79
147.36
147.19
146.77
135.94
135.79
135.47
135.42
135.32
135.27
129.84
129.78
129.72
129.47
129.13
129.04
128.99
128.47
120.15
120.10
119.90
119.84
117.83
117.81
117.73
117.70
77.38
77.07
76.75
42.51
40.99
30.98
30.92
A
B
C
D
CH2Cl
C-3C
C-3D
C-3'B
C-3A
C-3B
C-2C
C-2D
C-2A
C-2B
C-1C
C-1D
C-1A
C-1B
C-4A
C-4B
C-4C
C-4D
-C(CH3)2
-CH2-Cl
180
170
160
150
140
130
120
110
100
90
80
70
60
50
40
30
ppm

d)

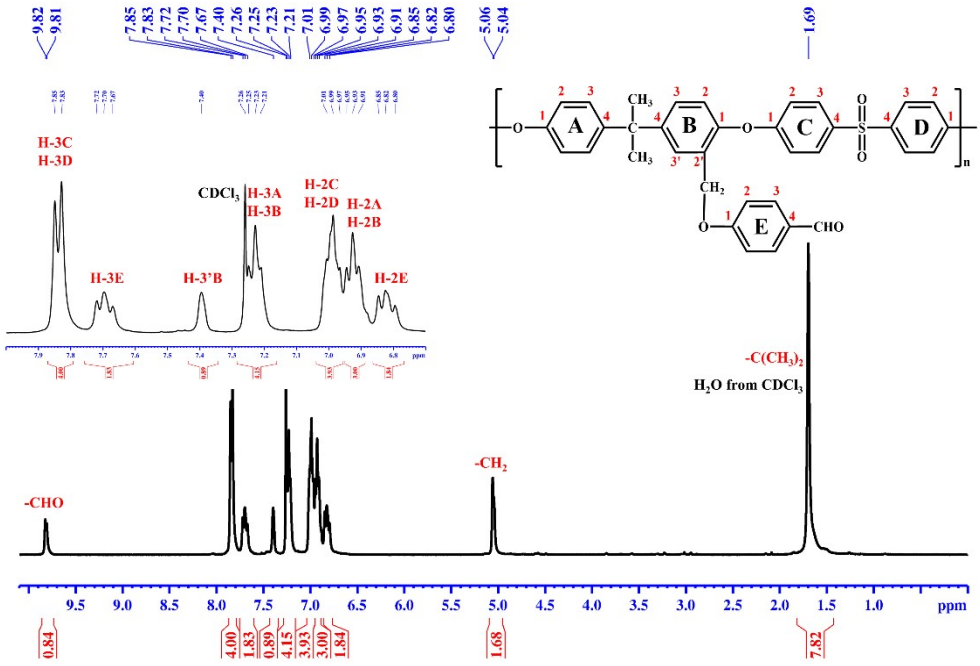
9.82
9.81
7.85
7.83
7.72
7.70
7.67
7.40
7.26
7.25
7.23
7.21
7.01
6.99
6.97
6.95
6.93
6.91
6.85
6.82
6.80
5.06
5.04
1.69
A
B
C
D
E
CHO
H-3C
H-3D
H-3E
H-3'B
CDCl3
H-3A
H-3B
H-2C
H-2D
H-2A
H-2B
H-2E
-C(CH3)2
H2O from CDCl3
-CH2
-CHO
9.5
9.0
8.5
8.0
7.5
7.0
6.5
6.0
5.5
5.0
4.5
4.0
3.5
3.0
2.5
2.0
1.5
1.0
ppm
0.84
4.00
1.83
0.89
4.15
3.93
3.00
1.84
1.68
7.82

e)

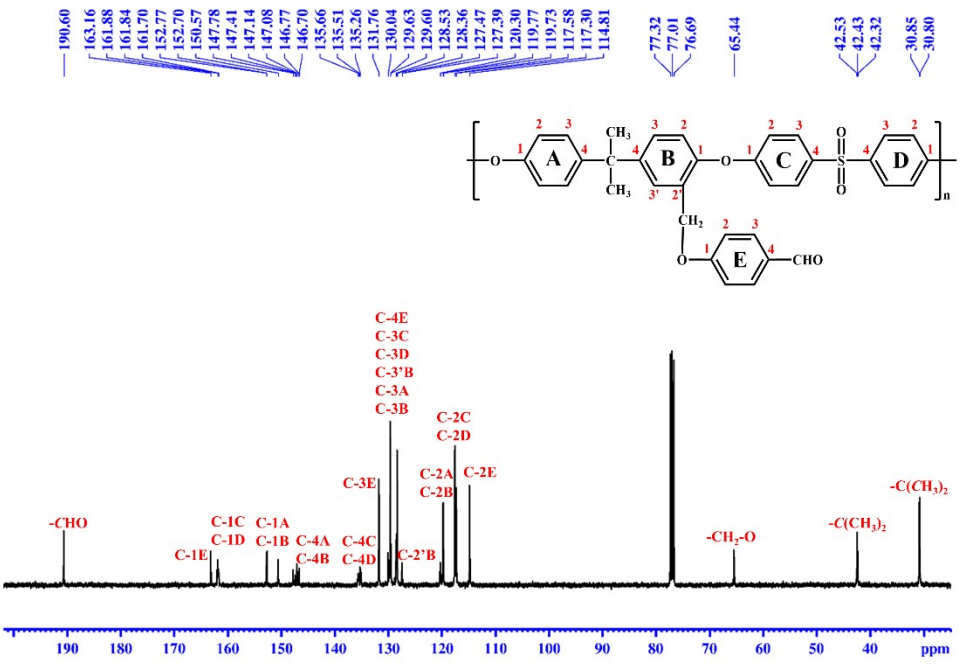

f)

Fig. S3. ^{1}H-NMR and ^{13}C-NMR spectra of PSF (a, b) CMPSF (c, d) and FPSF (e, f) with the inset in the ^{1}H-NMR spectra highlighting the overlapping of the signal of $C\underline{H}_3Cl$ which altered the value of the integral of aromatic protons from 3-C and 3-D

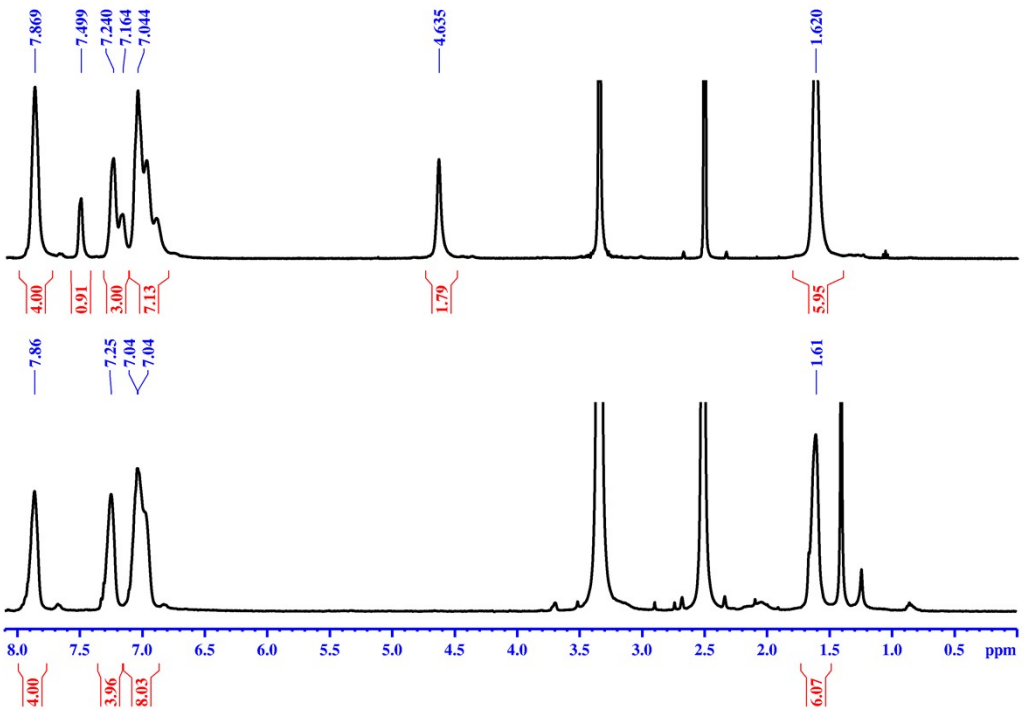

a)

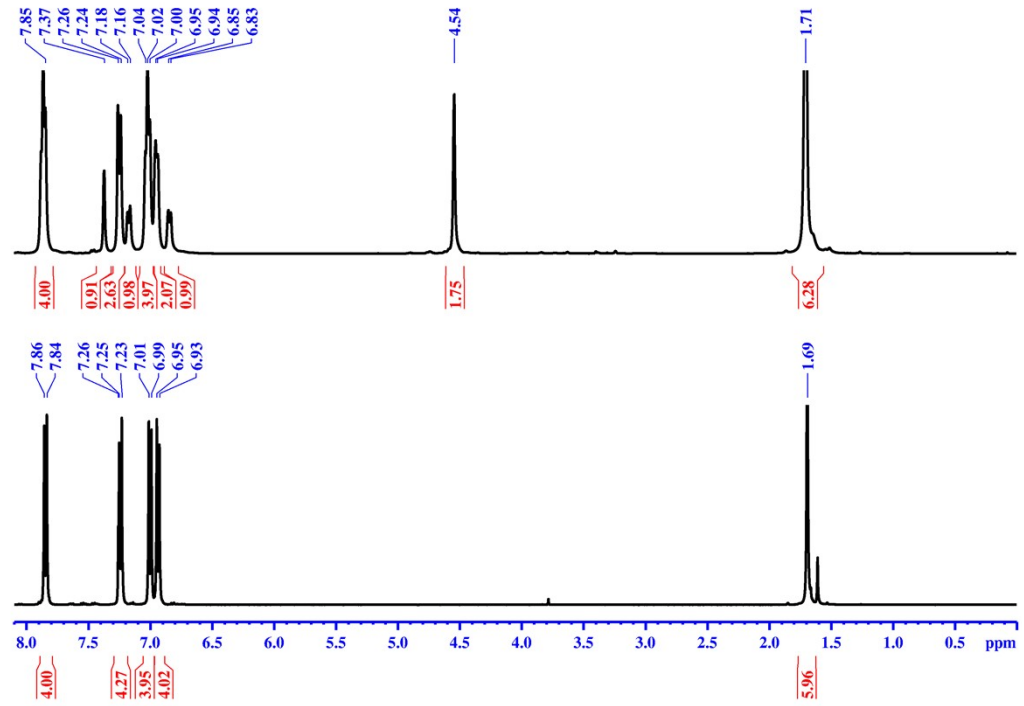

b)

Fig. S4. Comparative ^{1}H-NMR spectra of PSF and CMPSF recorded in a) DMSO d_6 and b) $CDCl_3$

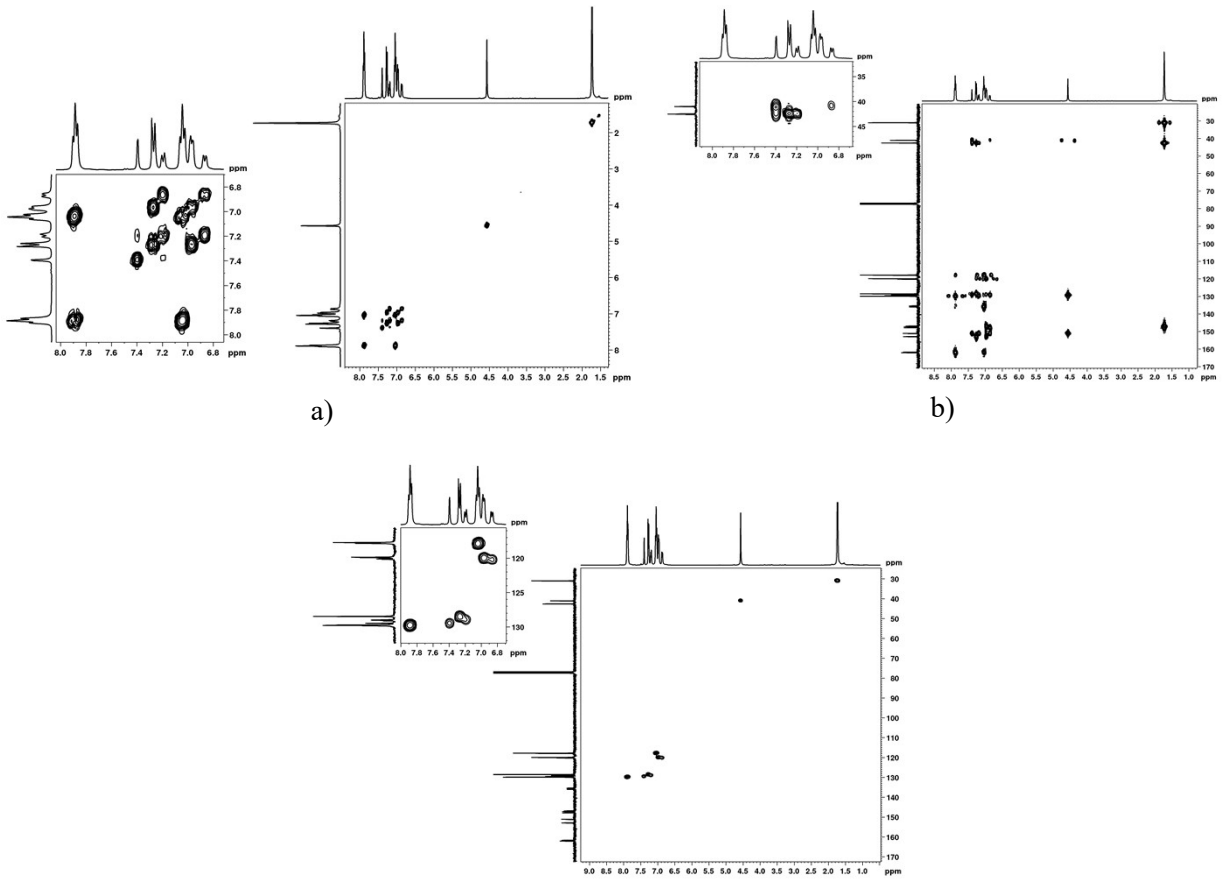

Fig. S5. Bidimensional NMR spectra: a) H-H COSY; b) H, C-HMBC; c) H, C-HSQC (The presence of long-range correlation signals between the C atom from CH_2Cl (40.9 ppm) and the proton H3'B (7.37 ppm) in the HMBC spectrum confirm the occurrence of substitution on the B aromatic ring)

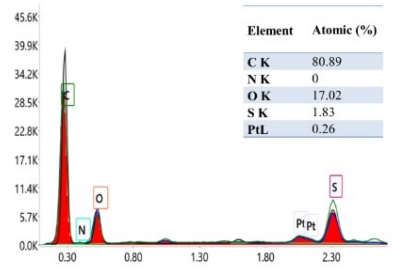

PS1

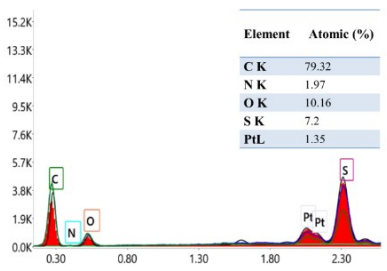

PS1I

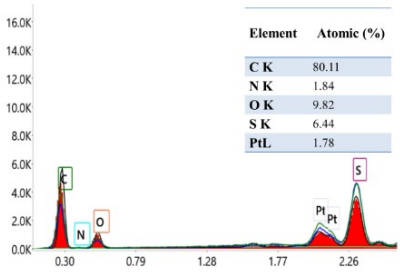

PS1R

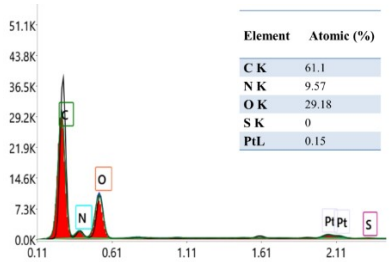

CS1

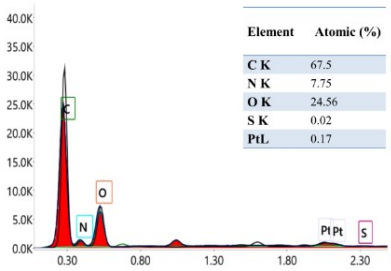

CS1I

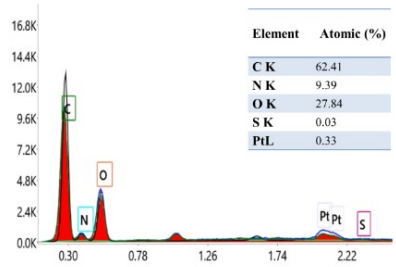

CS1R

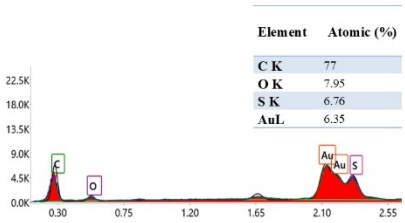

PS2

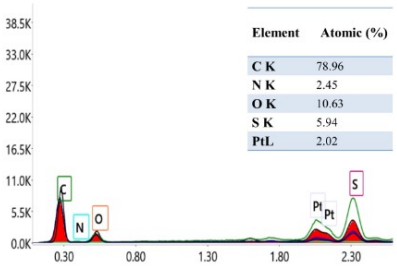

PS2I

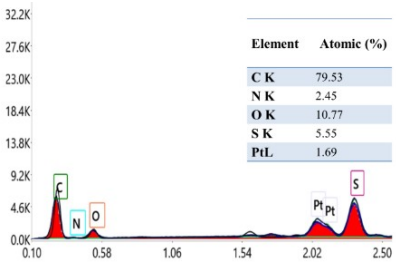

PS2R

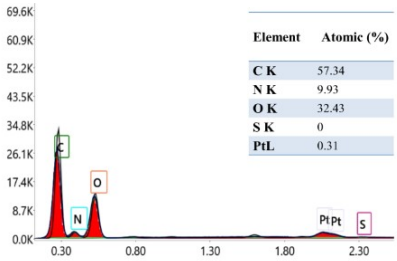

CS2

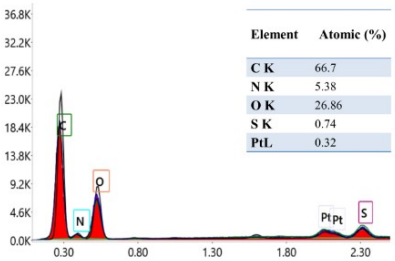

CS2I

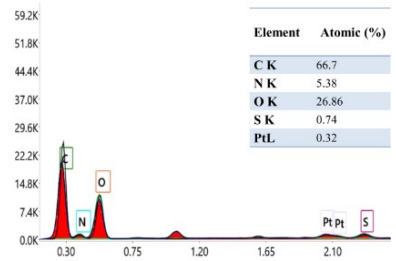

CS2R

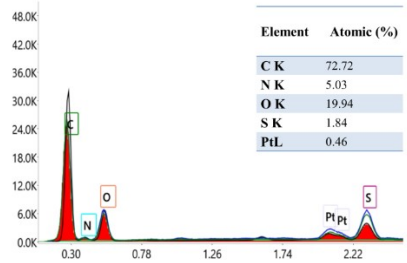

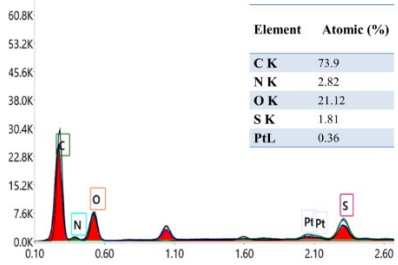

PS-CS-R

PS-CS-I

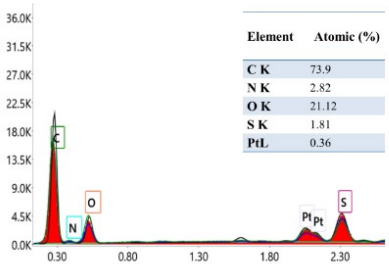

Element	Atomic (%)
C K	73.9
N K	2.82
O K	21.12
S K	1.81
PtL	0.36

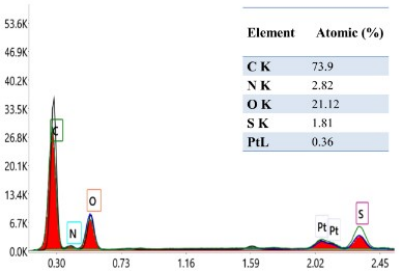

Element	Atomic (%)
C K	73.9
N K	2.82
O K	21.12
S K	1.81
PtL	0.36

CS-PS-I

CS-PS-R

Fig. S6. SEM-EDAX spectra of the investigated samples

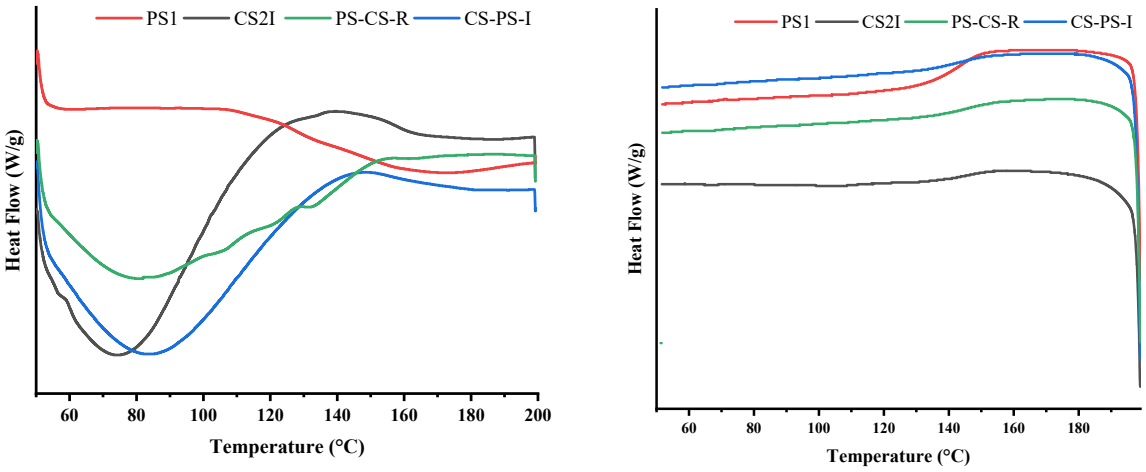

Fig. S7. DSC curves of several representative samples during a) heating and b) cooling scan

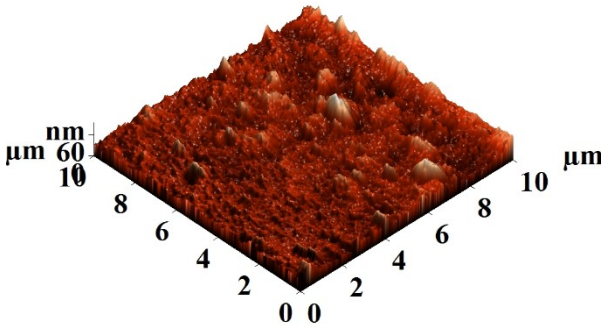

PS1

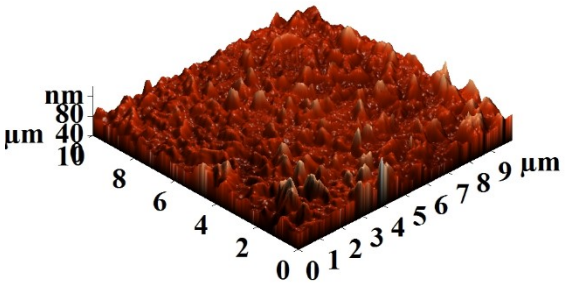

PS1I

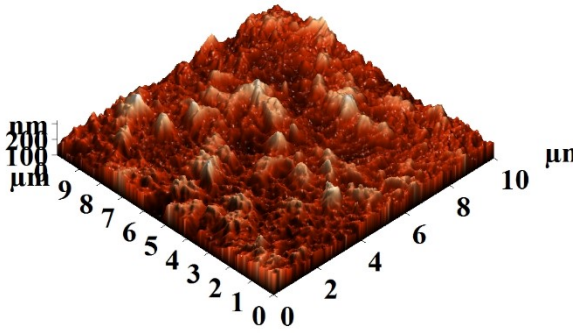

PS1R

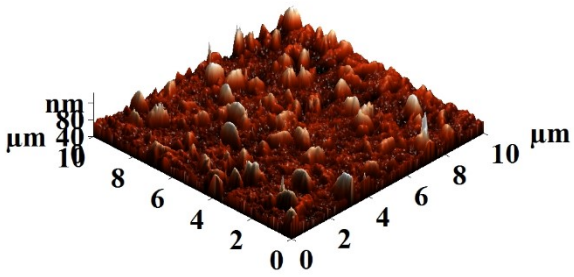

CS1

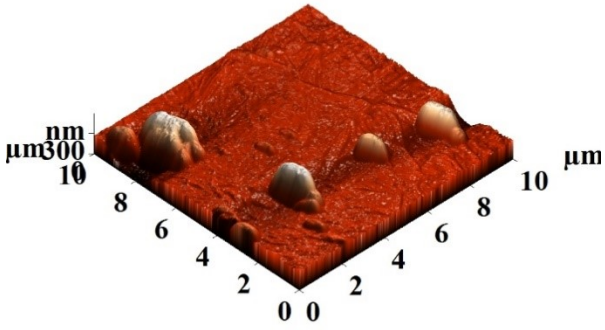

CS1I

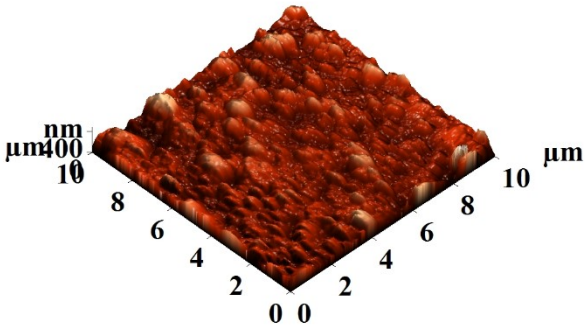

CS1R

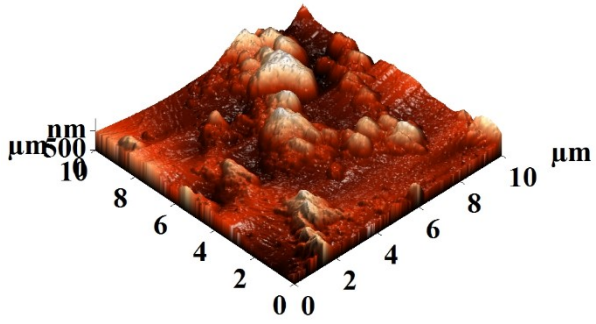

PS2

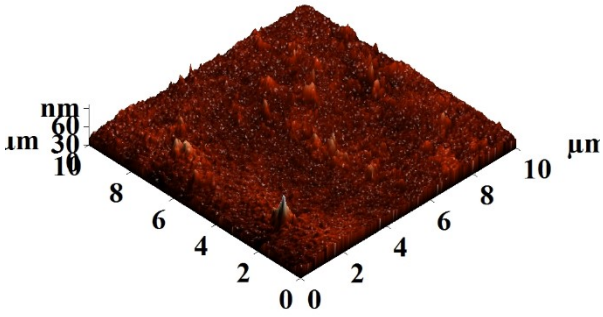

PS2I

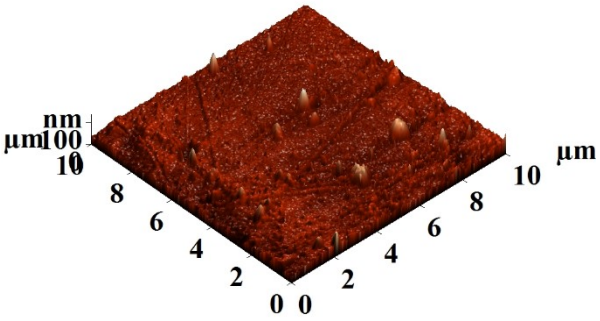

PS2R

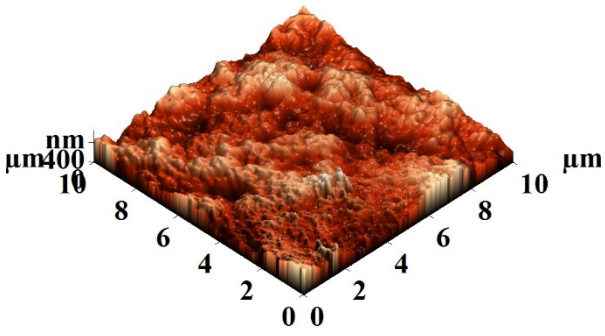

PS-CS-I

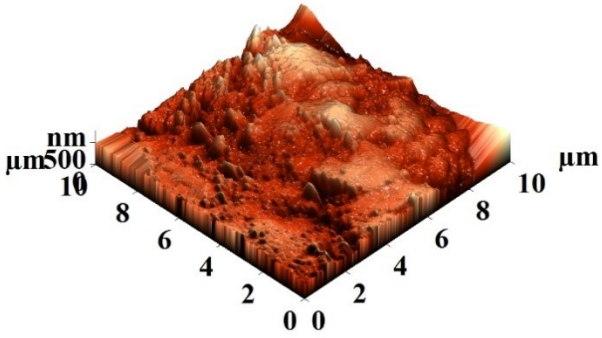

PS-CS-R

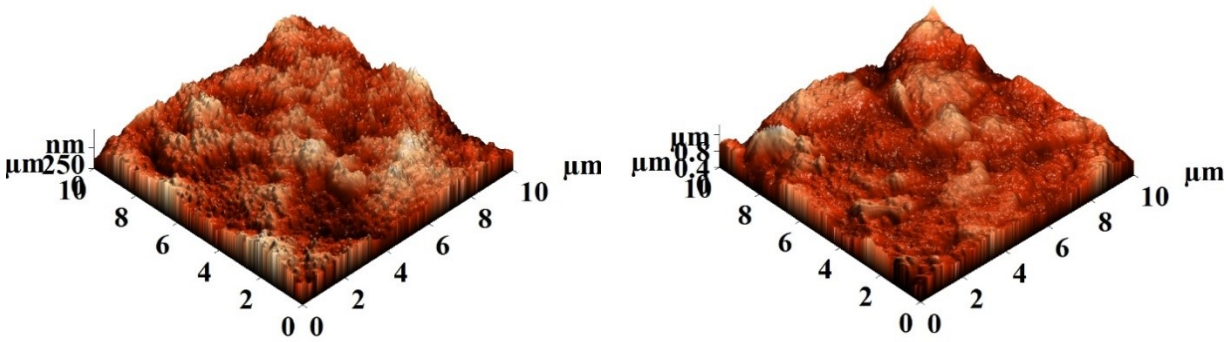

CS-PS-I CS-PS-R

Fig. S8. AFM images of the studied materials

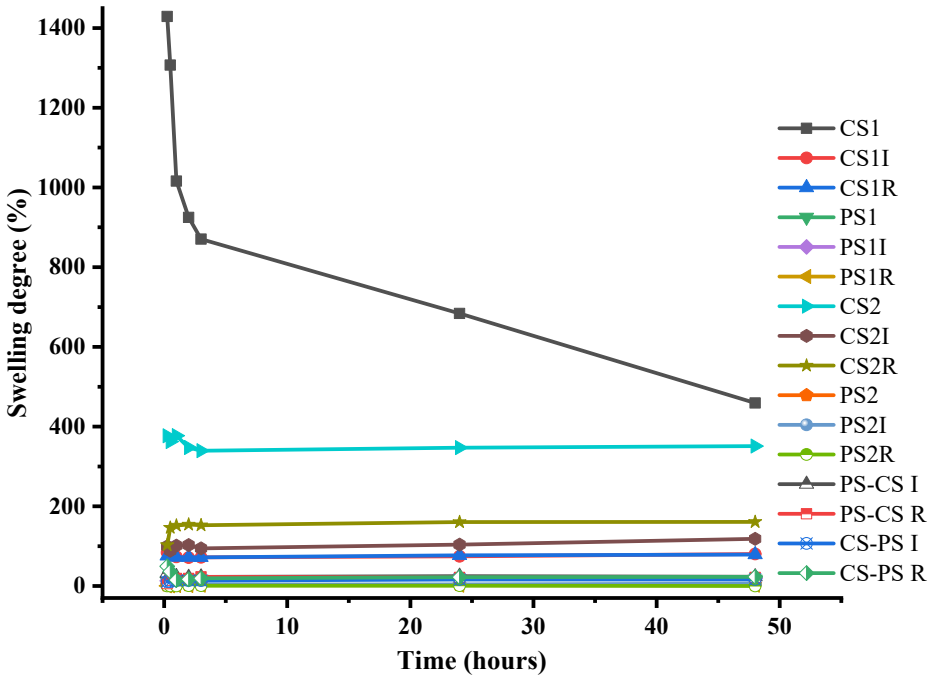

Fig. S9. The swelling kinetics of the investigated materials in PBS

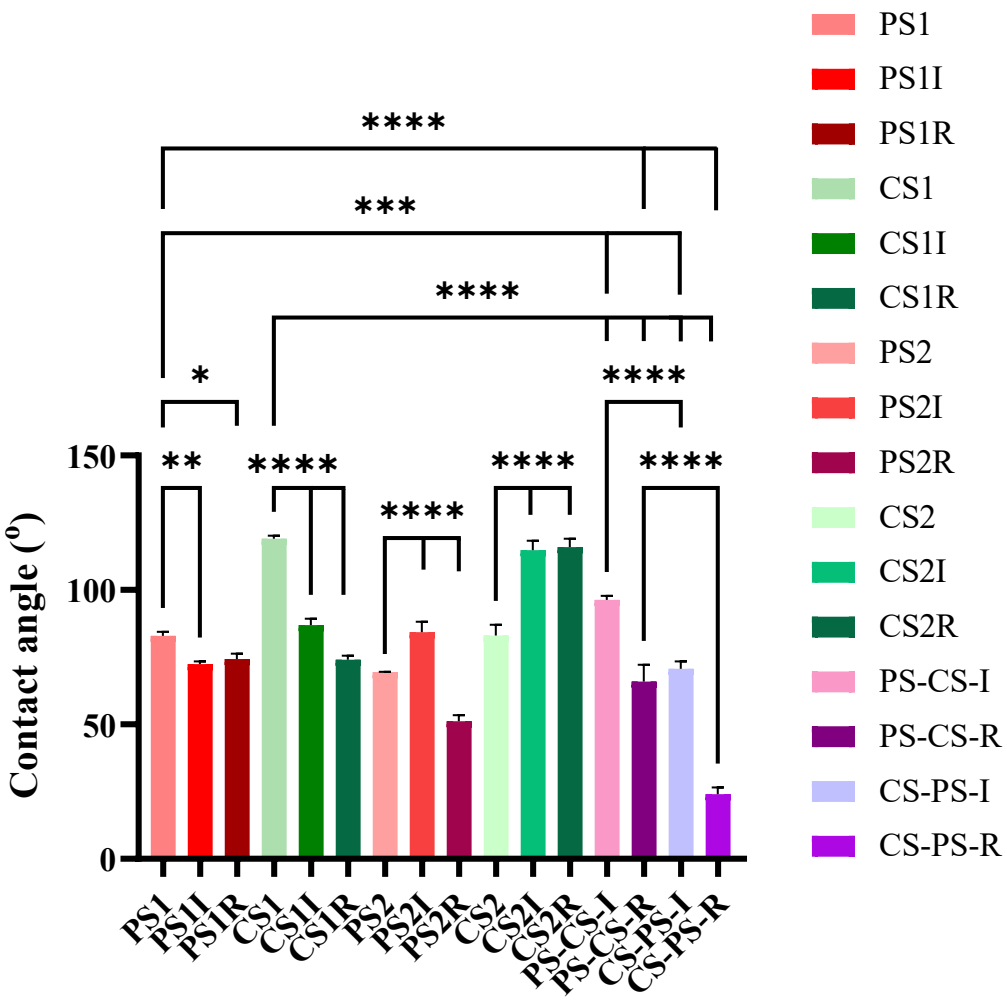

Fig. S10. Mean static contact angles of the samples with water determined by sessile drop method

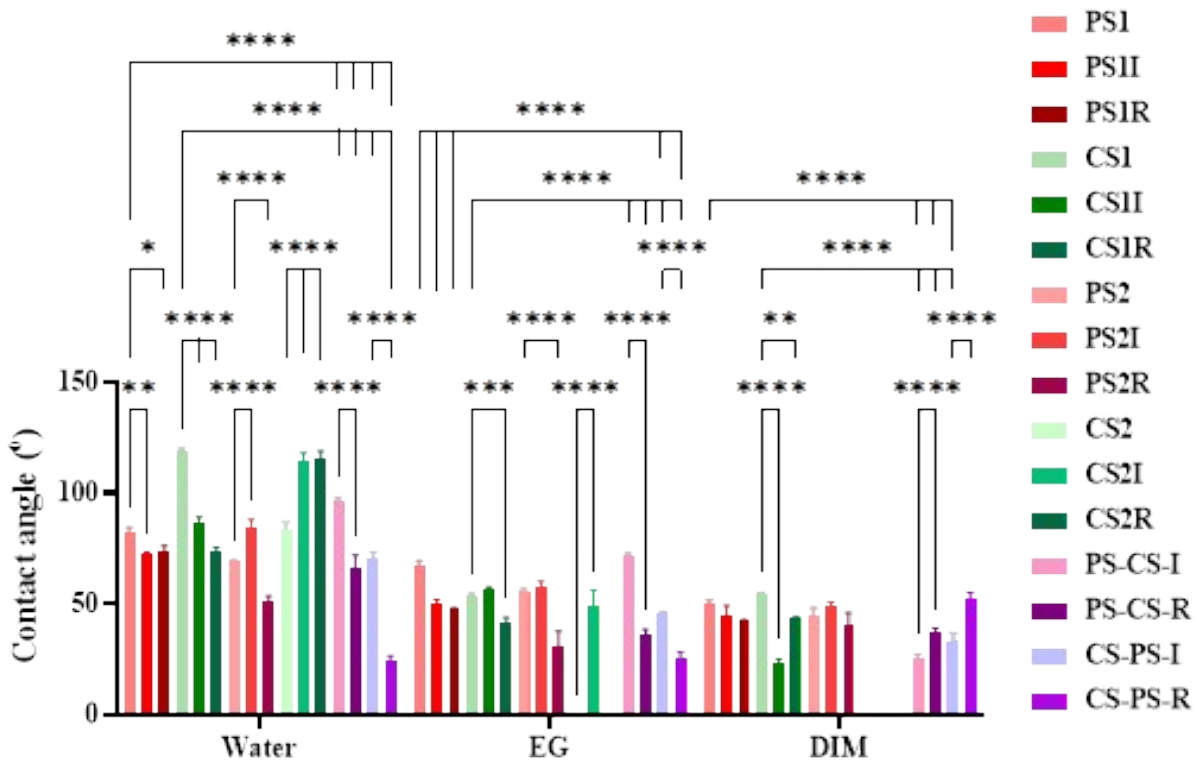

Fig. S11. Mean static contact angles of the samples with water, ethylene glycol and diiodomethane determined by sessile drop method

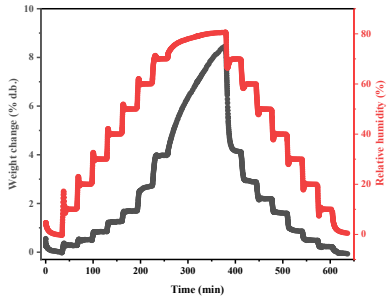

PS1

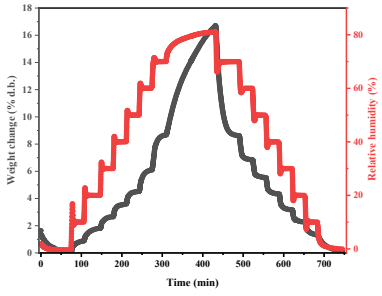

PS1I

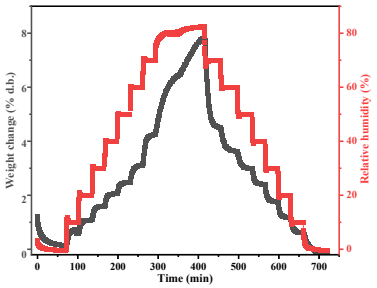

PS1R

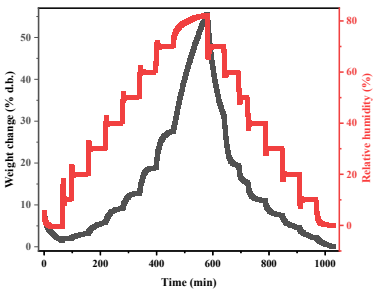

CS1

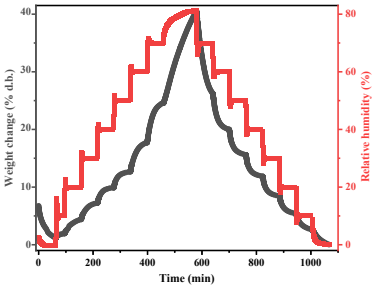

CS1I

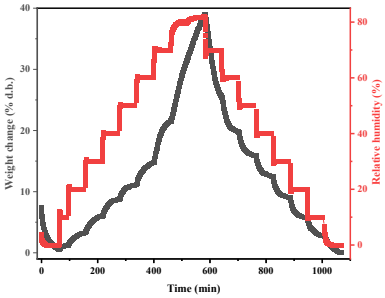

CS1R

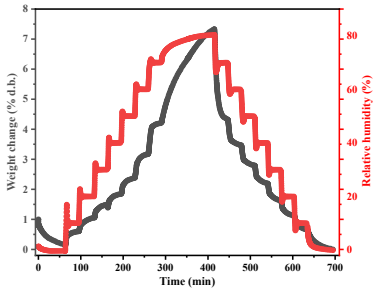

PS2

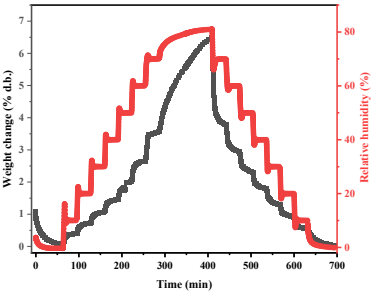

PS2I

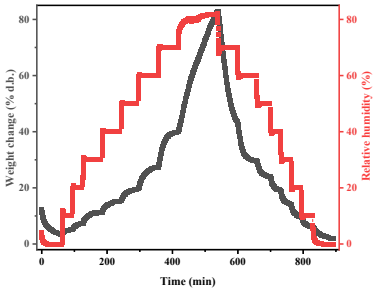

PS2R

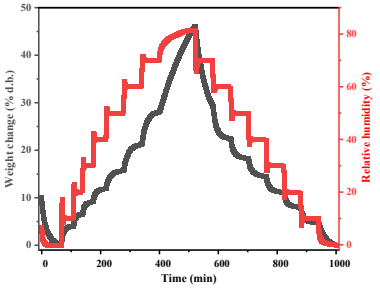

CS2

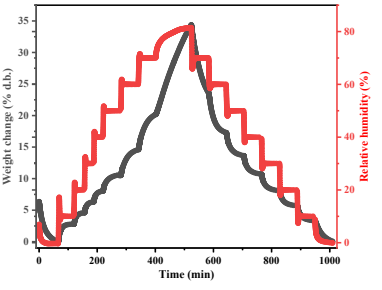

CS2I

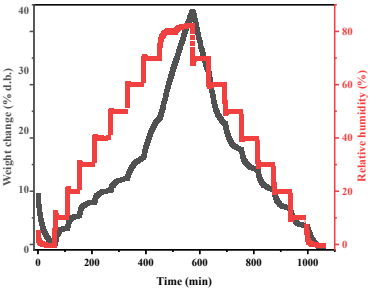

CS2R

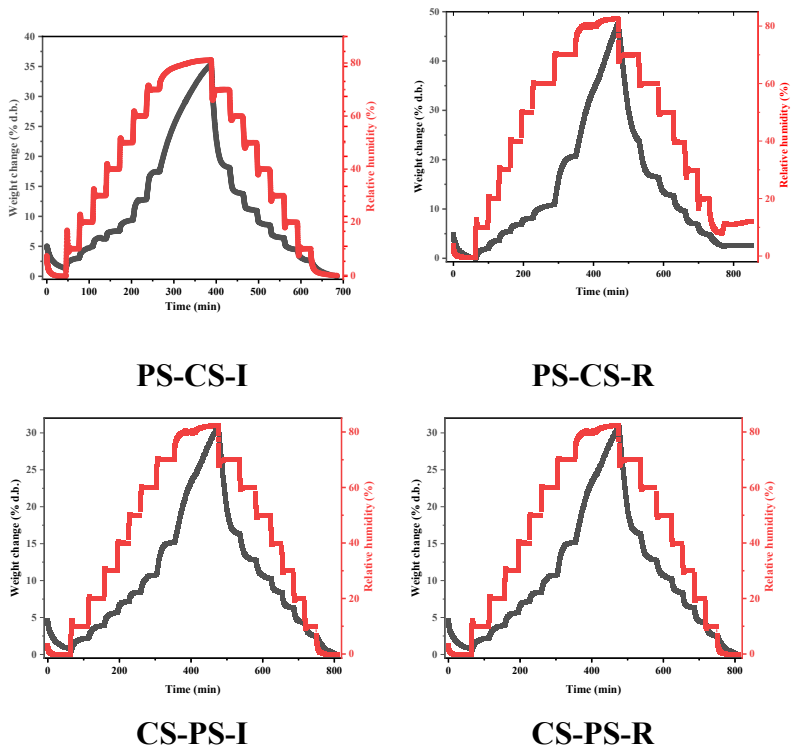

Fig. S12. Sorption desorption curves of the studied samples

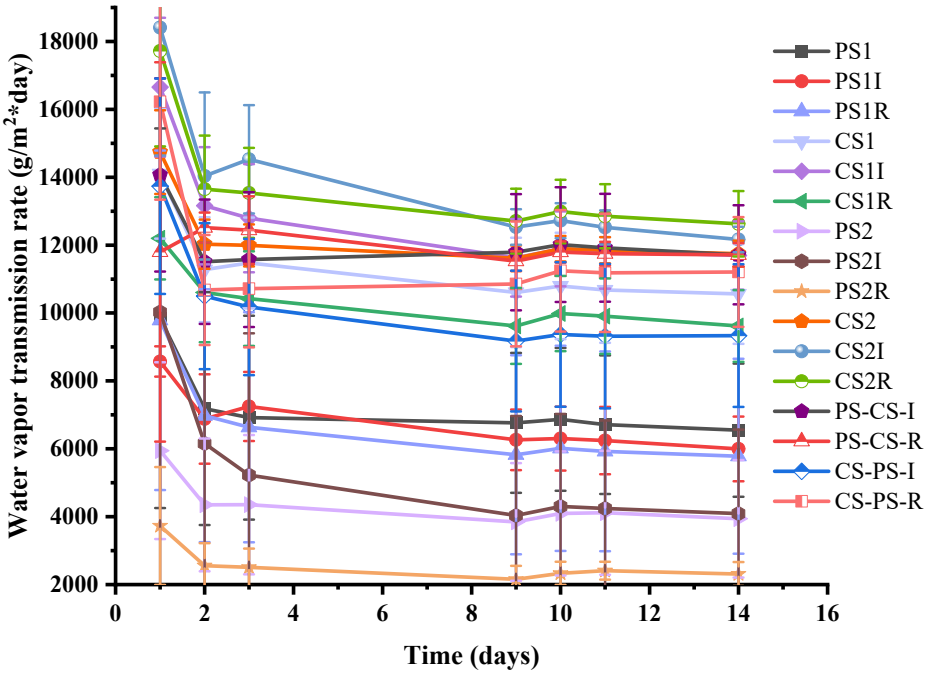

Fig. S13. Water vapor transmission rate evolution over 14 days of the investigated materials

Table S1. The diffraction angle and corresponding d-spacing of the studied materials

Sample	diffraction angle (2θ) / d-spacing (Å)					
PS1	-	5.06/17.46	-	-	18.02/4.97	
PS1I	-	4.88/18.10	9.5/9.33	-	18.2/4.93	
PS1R	-	4.76/18.55	9.08/9.75	-	18.5/4.85	
CS1	3.32/26.59	-	9.08/9.75	12.32/7.21	19.4/4.63	21.44/4.21
CS1I	-	4.58/19.28	9.44/9.38	15.38/5.80	-	20.36/4.42
CS1R	-	4.58/19.28	9.38/9.44	14.9/5.98	-	20/4.50
PS2	-	4.76/18.55	8.96/9.88	-	18.2/4.93	-
PS2I	-	5.18/17.05	9.32/9.50	-	18.14/4.94	-
PS2R	-	4.64/19.03	-	17.78/5.04	-	-
CS2	-	-	-	-	-	20.12/4.47
CS2I	-	4.94/17.88	-	-	18.86/4.76	-
CS2R	-	5.18/17.05	10.34/8.57	12.86/6.91	19.1/4.70	20.24/4.45
PS-CS-I	3.2/27.58	4.4/20.07	-	17.9/5.01	18.98/4.73	20.18/4.46
PS-CS-R	3.14/28.11	4.34/20.35	-		19.1/4.70	20.24/4.45
CS-PS-1	-	4.34/20.35	9.32/9.50	-	19.22/4.67	-
CS-PS-R	4.34/20.35	5.06/17.46	9.44/9.38	-	19.16/4.69	-

Table S2. Parameters of thermal degradation: maxima degradation temperatures (T_{max}) and corresponding mass loss, as well as the ash residue

Sample	T_{max} (ºC)	Mass loss (%)	Ash residue (%)
PS1	492	58.93	39.23
PS1I	510	52.87	42.54
PS1R	516	53.64	43.29
CS1	291	54.51	34.14
CS1I	500	9.27	35.731
CS1R	588	5.22	41.315
PS2	579	7.67	39.23
PS2I	510	46.48	42.54
PS2R	512	46.62	43.29
CS2	300	50.45	24.18
CS2I	509	14.19	33.18
CS2R	551	9.80	35.06
PS-CS-I	440	25.37	42.54
PS-CS-R	431	15.45	43.29
CS-PS-I	576	4.97	35.73
CS-PS-R	429	3.65	41.31

Table S3. Roughness average (R.a.) values in nm of the investigated samples, measured on surfaces of 5 × 5 μm^2 and 10 x 10 μm^2

Sample	R.a. (5x5)	R.a. (10x10)
PS1	5.93	6.96
PS1I	5.30	6.86
PS1R	16.60	19.32
CS1	6.75	7.37
CS1I	33.08	28.65
CS1R	40.13	47.18
PS2	60.06	97.54
PS2I	2.35	2.86
PS2R	4.45	5.92
CS2	15.87	-
CS2I	68.53	-
CS2R	15.87	-
PS-CS-I	58.93	77.18
PS-CS-R	43.88	71.64
CS-PS-I	34.09	50.14
CS-PS-R	31.17	85.90

- : Could not be recorded due to the porous morphology

Table S4. Surface free energy values (γ_{sv}) and disperse and polar components (γ_{sv}^{d}, γ_{sv}^{p}) for the investigated coatings in mJ/m^2

Sample	γ_{sv}^{d}	γ_{sv}^{p}	γ_{sv}
PS1	34.35	3.59	37.94
PS1I	37.30	7.03	44.33
PS1R	38.58	5.87	44.45
CS1	32.00	1.15	33.15
CS1I	46.72	0.86	47.31
CS1R	37.88	6.15	44.03
PS2	37.3	8.47	45.77
PS2I	34.59	3.12	37.71
PS2R	39.4	17.62	57.02
CS2	-	-	-
CS2I	-	-	-
CS2R	-	-	-
PS-CS-I	45.99	0.01	46.00
PS-CS-R	40.83	9	49.83
CS-PS-I	42.94	6.31	49.25
CS-PS-R	32.89	36.18	69.07

Table S5. Surface parameters of the investigated materials based on the sorption/desorption isotherms: sorption capacity (% d.b.), average pore size, specific surface area (m^2/g) and the amount of water retained in the monolayer (g/g).

			BET Data	
Code	**W (% d.b.)**	**rpm (nm)**	**Area (m^2/g)**	**Monolayer (g/g)**
PS1	8.461	0.736	229.632	0.065
PS1I	16.682	2.560	130.284	0.037
PS1R	7.902	2.328	67.871	0.019
CS1	55.526	2.397	463.184	0.131
CS1I	39.923	1.891	422.068	0.120
CS1R	38.942	1.623	479.622	0.136
PS2	7.332	2.510	58.405	0.016
PS2I	6.481	2.748	47.156	0.013
PS2R	20.426	3.080	132.603	0.037
CS2	45.964	2.381	386.002	0.109
CS2I	34.296	2.344	292.562	0.083
CS2R	39.799	2.097	379.454	0.108
PS-CS-I	35.347	3.031	233.226	0.066
PS-CS-R	47.360	1.756	539.137	0.153
CS-PS-I	30.733	2.682	229.162	0.065
CS-PS-R	34.327	2.595	264.465	0.075

References

[1] A. Warshawsky, N. Kahana, A. Deshe, H.E. Gottlieb, R. Arad-Yellin, Halomethylated polysulfone: Reactive intermediates to neutral and ionic film-forming polymers, J Polym Sci A Polym Chem 28 (1990) 2885–2905. https://doi.org/10.1002/POLA.1990.080281101.